Thermal and hydraulic performance of micro pin fin heat sinks with different pin fin shapes

IOP Conf. Series: Materials Science and Engineering **542** (2019) 012053 doi:10.1088/1757-899X/542/1/012053

Thermal and hydraulic performance of micro pin fin heat sinks with different pin fin shapes

Peng Wang[1], Liang Chen [2,3*]

1 Tianjin Key Laboratory for Civil Aircraft Airworthiness and Maintenance Airworthiness and Maintenance, Civil Aviation University of China, Tianjin 300300, China
2 Department of Mechanical & Electrical Engineering, Xiamen University, Xiamen, 361005, China
3 Shenzhen Research Institute of Xiamen University, Shenzhen 518000, China
E-mail: brightc66@163.com

Abstract. Efficient cooling of high heat flux devices has promoted the development of micro pin fin heat sinks. In this study, four micro pin fin heat sinks (MPFHSs) with different pin fin shapes, i.e., circular, square and diamond and streamline ones are fabricated by laser micromilling methods. Their single-phase heat transfer and fluid flow performance are explored to assess the pin fin shape effect. Convective flow tests are conducted at Reynolds number of 150-750 at two heat fluxes using deionized water as the coolants. It was found that the streamline MPFHS presented the best heat transfer performance. On the contrary, the diamond fin pin heat sink presented the worst heat transfer performance, whereas it featured the smallest pressure drop among the four MPFHSs. The diamond micro pin fins showed the smallest thermal resistance at a certain pressure drop, and should be selected as the optimum one for the MPFHS applications when the overall thermal and hydraulic performance is considered.

1. Introduction

The rapid development in the microelectronic technologies has promoted the miniaturization and high speed operation of electronic devices, e.g. projector, LED graphic chip, high power laser, etc. It induces a tremendous increase in power density, and results in serious thermal crisis [1]. Efficient cooling technologies are thus critical for the safe and reliable operation of electronic devices. Among them liquid cooling with micro pin-fin heat sinks (MPFHSs) is a promising solution [2]. The micro pin-fin heat sink features large surface area per given volume and low flow resistance, compact dimensions and small working fluid inventory requirements. Besides, the micro pin fins are helpful for the flow mixing and thermal and hydraulic boundary layer re-development, which introduces excellent heat transfer performance for solving high heat flux problems in electronic components [3]. Therefore, they have attracted increasing attentions in both research and industrial areas in recent years [4–6]. Many studies have been conducted to explore thermal and hydraulic performance of micro pin-fin heat sinks, and the applications in microelectronic chips[7], high-power LED lighting [8], turbine blades[9] have been also implemented.

Most of the works are focused on the heat transfer and pressure drop characteristics of a certain type of micro pin fins. The research groups of Peles et al. [10] comprehensively explored the convective flow performance of circular micro pin fins. The end-wall effect was found to contribute to a delay in flow separation for MPFHS. Besides, very low thermal resistances can be reached using a pin-fin heat sink. Lee et al. [6] experimentally studied the fluid flow and heat transfer of oblique pin fin heat sinks. A parametric study involving the oblique angle, fin pitch is also carried out. Notable heat transfer augmentation was reached for these oblique pin fin heat sinks with maximum heat transfer performance enhancement at 47% compared to conventional straight microchannels. Liu et al. [11] investigated the convective liquid flow and heat transfer performance of micro square pin fin heat sink using water. High heat transfer coefficient was obtained with water single-phase flow in micropin-fin arrays, suggesting

that micropin-fin heat sinks can be very effective meeting the needs of many high-heat-flux electronic cooling applications.

Besides, the effects of arrangement patterns and aspect ratios on the thermal performance of MPFHSs are also explored. Jeng et al. [12] experimentally studied the pressure drop and heat transfer of a square pin-fin array in a rectangular channel with different relative longitudinal pitch, relative transverse pitch and pin fin arrangements (in-line or staggered). It was found that the staggered pin-fin array presented larger pressure drop. The optimal inter-fin pitch and transverse pitch are also given. Roth et al. [13] found that the staggered pin fin arrangement enhanced heat transfer for 56% compared to corresponding in-line arrangement, which should be selected for efficient cooling applications. Moreover, Rasouli et al. [14] explored pitch and aspect ratio effects on single-phase liquid flow and heat transfer of micro pin fin heat sinks together with flow visualization. Unsteady vortex shedding in the micro pin fins were also found, which played a notable role on the heat transfer performance.

From the above literature review, most of the previous studies of micro pin fins were focused on the thermal and hydraulic performance of a certain type of micro pin fins, or MPFHSs with different arrangement patterns and aspect ratios. The micro pin fin shapes may play a notable role on the thermal and hydraulic characteristics of MPFHSs, which has been pointed out in the studies of silicon MPFHS with circular, rectangular, hydrofoil and cone-shaped micro pin-fins by Kosar and Peles [3] . Nevertheless, the information for the MPFHSs with different pin fin shapes are far from sufficient, especially for the MPFHSs with metal micro pin fins. To this aim, we fabricated four kinds of micro pin fins with different shapes, i.e., square, diamond, circular and streamline ones in copper to build copper micro pin fin heat sinks. Fluid flow and heat transfer performance of these four MPFHSs were explored and compared for the design optimizations.

2. Experiments

2.1 Fabrication of micro pin fins

The micro pin fins are fabricated by a laser micromilling method on pure red cooper plates (99.9% Cu) with the dimensions of $45 \times 20 \times 2$mm (length $\times$ width $\times$ height). Laser micromilling, as a non-contact and highly precise microfabrication technique, can fabricate a part via laser ablation by controlling the materials removal. A prototype pulsed fiber laser (IPG, No: YLP-1-100-30-30- HC-RG, Russia) system is utilized, and the cross machining route and loop multiple-pass reciprocating scanning strategy are adopted to process the micro pin fins. The laser is set to produce 100 ns pulses with a 1064nm fundamental wavelength (λ) at a repetition rate of 20kHz. All the micro pin fins are fabricated at the same processing parameters, i.e., the laser output power of 27W, scanning speed of 250mm/s and scanning times of 20.

Fig.1 shows the fabricated micro pin fin heat sinks with different pin fin shapes, i.e., square, diamond, circular and streamline ones. They are in staggered arrangements. All the micro pin fins are fabricated in the center of copper plate with the dimensions of 17×45mm ($W_{ht} \times L$, W_{ht} and L are the width of heat transfer area and length of heat sink, respectively). The geometric dimensions of these micro pin fins are shown in Table.1.

Table 1 Geometric parameters of four micro pin fins samples

Pin shape	Circular	Square	Diamond	Streamline
Length of a micro pin fin, L_{fin}, (mm)	0.5	0.5	1.5	0.5
Width of a micro pin fin, W_{fin}, (mm)	0.5	0.5	0.4	0.5
Longitudinal pitch, S_L, (mm)	1.5	1.5	3.43	1.5
Transverse pitch, S_T, (mm)	1.5	1.5	0.92	1.5
Cross-sectional area of a single micro pin fin, A_{fin}, (mm^2)	0.196	0.25	0.3	0.297
Number of rows, N_{row}	13	30	30	30
Number of pin fins in a single row, N_s	35	22	22	22

Total number of micro pin fins, *N*	660	660	455	660

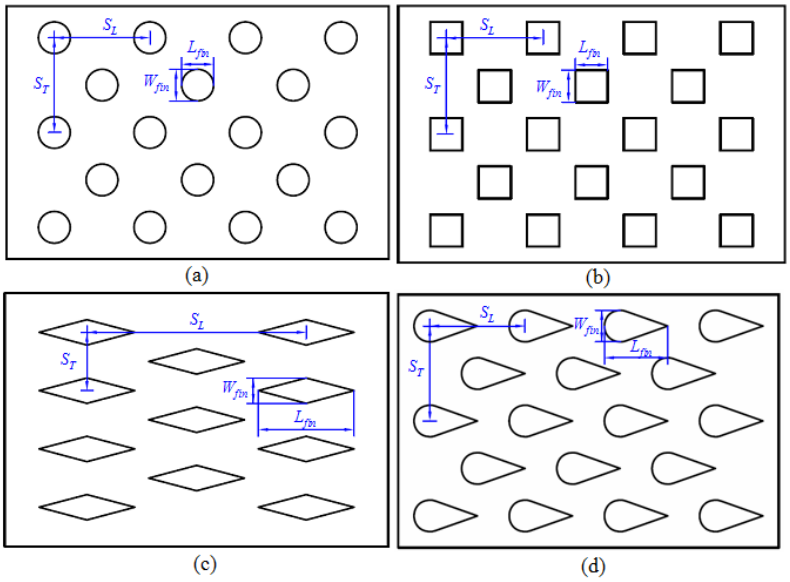

Figure 1 Illustrations of the four micro pin fins: (a) circular; (b) square; (c) diamond (d) streamline

2.2 Description of the test system and procedure

The convective flow test system is similar to that in the previous study [5], which is described here briefly. The experimental test loop is composed of a water tank, a magnetic gear pump, a filter and valves, a micro turbine type flowmeter, a constant temperature water bath and heat exchanger, MPFHS test section and heating modules, a microscope together with high-speed camera for flow visualization and data acquisition system. The MPFHS test section consists of the micro pin fin samples, copper block heating module, inlet and outlet plenums, a Pyrex glass cover plate, a polyetheretherketone (PEEK) flow housing, an assembling top plate and insulating components, as shown in Fig.2. The heating copper block with cartridge heaters inside consists of an upper rectangular section of 20x45mm, which is identical to footprint dimensions of micro pin fin samples. The micro pin fin sample is soldered on top of the copper block using a 0.5mm thin layer of solder (Pb-Sn-Ag-Sb, k_s=50W/m ·K) to minimize the contact thermal resistance. Any possible leakage of coolants around the periphery of heating copper block is prevented by utilizing RTV silicone rubber in the interface of copper block and flow housing. Good insulation of heating copper block is maintained as it is wrapped by the PEEK insulating block with low thermal conductivities. The assemblies of cover plate, glass cover, microchannel sample, flow housing and insulating block are clamped together by screws with an O-ring to ensure the good contact between the glass cover and the top surface of micro pin fins.

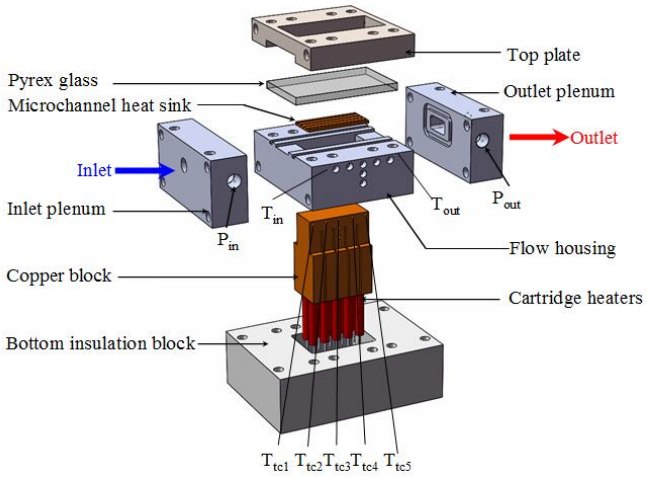

Figure 2. Schematic of the cross-section of test section.

The test section is heated by ten cartridge heaters with the maximum total power of 1000W. Five K-type shielded thermocouples of the diameter of 1mm are embedded in the copper block at a distance of 2mm below the top surface of copper block to measure the stream-wise wall temperature distribution of micro pin fins. The locations were 2.5, 12.5, 22.5, 32.5, 42.5mm, respectively, from the channel inlet position. The inlet, outlet temperatures are monitored by type-K thermocouples, and the inlet and outlet pressure during the test are measured by two pressure transducers with a response time of 3 ms. All the temperatures and pressure drop data are collected by an Agilent 34970A data acquisition system.

In this study, deionized water is utilized as the test coolant. The water is fully degassed via vigorous boiling for about half an hour prior to each experimental run. Tests are conducted for all the MPFHS samples at inlet temperature of 33 ℃ and two heat fluxes levels (133 and 267kW/m^2) in atmospheric conditions. The supplied power and inlet temperature are maintained to be constant, and differentf coolant flow rates are supplied by adjusting the flowmeter. When the wall temperatures are fluctuated within 0.5 ℃, the steady state is thought to be reached. Then all temperature and pressure data are recorded at 1 s interval for 2 min. The heat transfer and pressure drop data can thus be calculated by the averaged values of measurement results for all the period of 2 min.

2.3 Theoretical background and data reduction

The sensible heat gained by the coolant can be determined from the energy balance,

$$q_{eff} = \rho c_p \dot{V}(T_{out} - T_{in}) \tag{1}$$

where $\dot{V}$ is the volumetric flow rate, T_{in} and T_{out} is the inlet and outlet coolant temperatures, respectively. c_p and ρ are the specific heat and density of coolant, respectively.

The average convective heat transfer coefficient can be obtained by Newton's law of cooling,

$$h = \frac{q_{eff}}{(\overline{T_w} - \overline{T_f})A_{ch}} \tag{2}$$

where $\overline{T_f}$ is the average of the inlet and outlet coolant temperatures,

$\overline{T_w}$ is the average wall temperature of the five thermocouples locations along the microchannel,

$$\overline{T_w} = \frac{T_{w,tc1} + T_{w,tc2} + T_{w,tc3} + T_{w,tc4} + T_{w,tc5}}{5} \tag{3}$$

The wall temperatures of microchannels ($T_{\text{w,tci}}$) at the thermocouple locations are derived from one dimensional Fourier's heat conduction equation. They are given in detail in a thermal resistance network in the previous study [15], and are given as follows

$$T_{w,tci} = T_{tci} - q_{eff}\left(\frac{l_{Cu}}{k_{Cu}A_t} + \frac{l_{hs}}{k_m A_t} + \frac{l_s}{k_s A_t}\right) \tag{4}$$

where T_{tci} is the local thermocouple reading(i=1-5), k_{Cu}, k_s, k_m were the thermal conductivities o f copper, solder and the MPFHS base, respectively. l_{Cu} and l_s are the distances from the thermocoupl e location to the top heating surface of copper block and thickness of solder, respectively. l_{hs} denotes t he distance between the backside surface of MPFHS sample and bottom surface of micro pin fins. A_{ch} is the total heat transfer area of MPFHS, which can be calculated using the approaches detailed in Ref. [5].

After the cacaulation of convective heat transfer coefficient, the Nusselt number cna be deterimined by,

$$Nu = \frac{hD_h}{k_f} \tag{5}$$

in which D_{h} is the hydraulic diameter, which is cacaulated as follows,

$$D_h = \frac{4A_c L}{A_t} \tag{6}$$

where A_t is the total surface area in contact with coolants, A_c is the minimum cross-section free flow area, L is the length of MPFHS sample.

The Reynolds number is expressed as

$$\mathrm{Re} = \frac{\rho u D_h}{\mu} \tag{7}$$

where ρ , μ , u are the density, dynamic viscosity of the fluid, average flow velocity, respectively.

The total thermal resistance of MPFHS is defined as

$$R_t = \frac{T_{\max} - T_{in}}{q_{eff}} \tag{8}$$

where $T_{\max}$ is the maximum measured temperature of the five thermocouples in the stream-wise direction, T_{in} is the inlet coolant temperature.

Uncertainties in individual temperature measurements are $\pm 0.3℃$ for the type-K thermocouples. The maximum errors for the flow meter and pressure transducer are 2% and 0.1% of full scale, respectively. The supply power measured by the digital power meter yield an uncertainty of 1%. Using the standard error analysis method [16], the maximum uncertainties in the Nusselt number and pressure drop can be estimated to be 7.5%, 5.4%, respectively.

3. Results and discussion

3.1 Heat transfer performance

Fig.3 shows the average Nusselt number as a function of the varation of Reynolds number in both heat fluxes cases. Generally, all the MPFHS samples presented a monotonic increase trend in Nu with increasing Re, as the thermal boundary layer tended to be thinner when the fluid velocity increased. For the three MPFHSs with circular, square and diamond micro pin fins, when the flow velocity was low with small Reynolds number, there are no notable differences among circular, diamond and square pin fin heat sinks. This can be related to that these MPFHSs featured thick boundary layers in small flow rates, and the cross-sectional shapes did not played s significant role on the heat exchange process. Nevertheless, when the Reynolds number increased to larger than about 250, the Nu~Re curves of the circular, diamond and square pin fin heat sinks tend to diverge from each other. The cross-sectional pin fin shapes showed a remarkable role on the heat transfer performance. The square pin fin heat sinks showed a fast rise in the Nu, and outperformed other two MPFHSs. The square pin fins seemed to facilitate the heat transfer process from pin fin walls to coolants. The following is the circular ones, and the diamond MPFHS presented the worst heat transfer performance.

For the entire test range of flow rates, the streamline MPFHS presented the best heat transfer performance among all the four MPFHSs. For example, at the test conditions with Re of about 400 in heat flux of 133kW/m^2, the streamline MPFHS present a Nu of 9.6, which is 32% larger than the square one, and 68% larger than the circular one. The streamline MPFHS enhanced the heat transfer for even 142% compared to the diamond one. As can be seen in Fig.1, the streamline micro pin fins featured circular portions in the head and triangular tails. The circular upstream head may induce intense flow disruptions and separations, which contributed to more flow mixing and enhancement in the convection heat exchange. Moreover, the triangular tails reduced the occurrence of vortices , as the separated flow can flow quickly along the long pin fin surface to the downstream. Therefore, they present the good heat transfer performance.

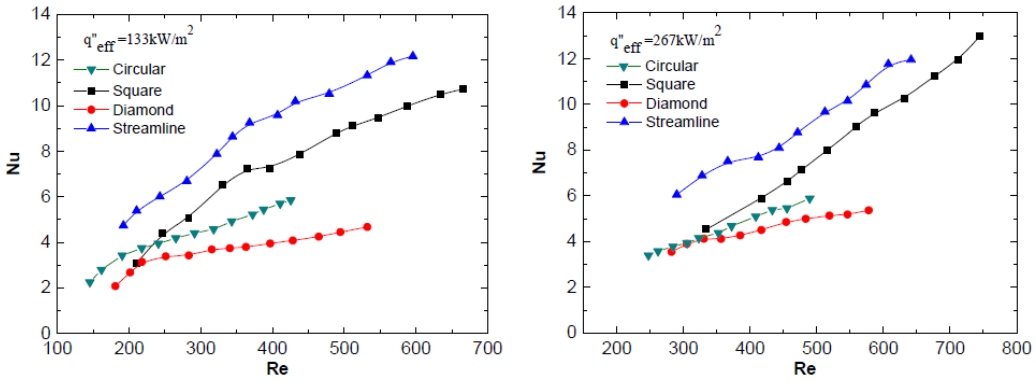

(a) (b)

Figure 3 Average Nusselt number for MPFHS samples with different pin fin shapes: (a) q''eff =133kW/m^2; (b) q''eff =267kW/m^2.

3.2 Pressure drop

Fig.4 shows the pressure drop characteristics of four micro pin fin heat sinks at two levels of heat fluxes. All the samples presented a monotonic increase trend in pressure drop with increasing Reynolds number, as larger flow rate cases resulted in larger friction loss during the fluid flow in micro pin fins. This is consistent to the results of many other reports [6, 11]. For all the four MPFHSs with different cross-sectional shapes, it can be noted from Fig.4 that the circular pin fins showed the largest pressure drop penalty. This may be attributed that the circular pin fins without no protrusions or corners induced faster local flow velocities inside the micro pin fin flow passages, which resulted in the larger frictional drag and large pressure drop. Following is the streamline and square ones. The diamond fin pin heat sinks presented the smallest pressure drop. For example, at the test conditions with Re of about 400 in heat flux of 133kW/m^2, the $\triangle P$ of diamond MPFHS was just 1.25kPa, which is 42% smaller than the square one, 58% smaller than streamline one, and even 80% smaller than the circular one. The notable reduction in $\triangle P$ for diamond MPFHS can be related to the fact that the small protruded head facilitated to separate the main flow into two portions of flow, which reduced the collision between coolants and pin fins. This reduced the shear forces between coolants and pin fin walls, and induced the smallest form drag. Therefore, the smallest pressure drop can be noted for diamond micro fin pin heat sinks.

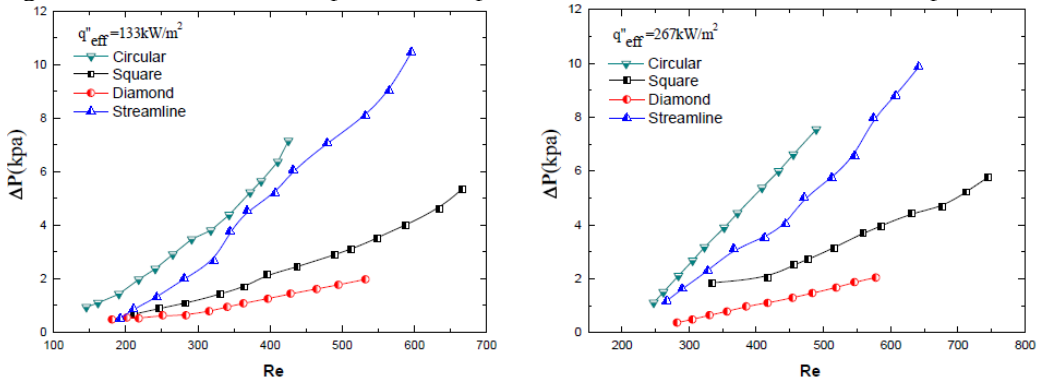

(a) (b)

Figure 4 Measured pressure drop for MPFHS samples with different pin fin shapes: (a) q''eff =133kW/m^2; (b) q''eff =267kW/m^2.

3.3 Thermal resistance and overall performance comparison

To combine the evaluation of heat transfer and pressure drop characteristics of the heat sinks, the total thermal resistance was often assessed and compared with each other under the constant of pressure drop [10, 17]. Fig.5 shows the thermal resistance of all the MPFHS samples versus the pumping power in both heat fluxes tests. When the pressure drop increased together with the flow rates and Reynolds

numbers, the total thermal resistance of all the MPFHS samples firstly decreased quickly, and then flattened out at large pressure drop which is linked to large flow rates conditions. As the heat transfer performance of the MPFHS samples increased considerably at large flow rates cases as mentioned before, the thermal resistance can be lowered down with the rise in flow rates.

For the four MPFHS samples with different pin fin shapes, it can be noted from Fig.5 the circular one generally presented the worst thermal performance with the largest thermal resistance, as it accompanied with the largest pressure drop. Followed is square and streamline ones. Despite that the streamline MPFHS presented the best heat transfer performance, its large pressure drop may play a negative role on the overall performance of MPFHS. The diamond micro pin fin heat sinks, however, present the smallest thermal resistance at the same pressure drop. Such behavior is in line with the pressure drop trends, and can be associated to the dominance of pressure drop in the R_t~△P curves [10]. Even though the diamond MPFHS showed the smallest heat transfer coefficients, it present much smaller pressure drop than other three samples. The significant decrease of pressure drop for the diamond MPFHS contributed to the lowest thermal resistance in the R_t~△P curves. Therefore, the diamond micro pin fins should be selected as the optimum one for the MPFHS applications when the overall thermal and hydraulic performance is considered. Nevertheless, if the heat transfer performance is of the prior considerations, the streamline one should be selected as the optimum one.

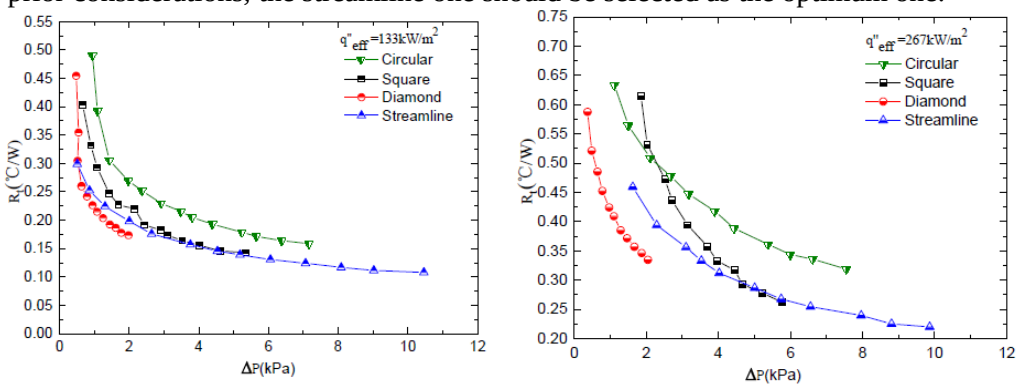

(a) (b)

Fig. 5. Thermal resistance against pressure drop for MPFHS samples with different pin fin shapes: (a) q''eff =133kW/m^2; (b) q''eff =267kW/m^2.

4. Conclusions

In this study, micro pin fin heat sinks with four different micro pin fin shapes were developed. Their thermal and hydraulic characteristics were assessed using water at two heat fluxes. It was found that the streamline MPFHS presented much lager Nusselt number, and presented the best heat transfer performance. The micro pin fin shapes firstly showed no notable effects on the heat transfer performance of circular, square and diamond MPFHS at small flow rates, but they began to play a significant role on the Nu when the Re increased to be larger than about 250. The circular pin fins showed the largest pressure drop penalty, followed by streamline and square ones. The diamond fin pin heat sinks presented the smallest pressure drop. The overall thermal and hydraulic performance in terms of total thermal resistance as a function of pressure drop generally followed the order of diamond, streamline, square and circular MPFHSs. The diamond micro pin fins should be selected as the optimum one for the MPFHS applications when considering the overall thermal and hydraulic performance.

Acknowledgments

The research was financially supported by and the Science and Technology Planning Project of Guangdong Province, China (No. 2017A010104002), and the open fund of Tianjin Key Laboratory for Civil Aircraft Airworthiness and Maintenance Airworthiness and Maintenance.

References

[1] Tang H, Tang Y, Wan Z, Li J, Yuan W, Lu L, Li Y, Tang K. Review of applications and developments of ultra-thin micro heat pipes for electronic cooling. 2018 *Appl. Energy* **223**,383–400
[2] Mohammadi A, Koşar A. Review on Heat and Fluid Flow in Micro Pin Fin Heat Sinks under Single phase and Two phase Flow Conditions. 2018 *Nanoscale Microscale Thermophys. Eng.* **22**,153-197
[3] Kosar A, Peles Y, Micro Scale pin fin Heat Sinks—Parametric Performance Evaluation Study. 2007 *IEEE Trans. Compon. Packag. Tech.* **30,** 1-11.
[4] Qu W, Siu-Ho A, Experimental study of saturated flow boiling heat transfer in an array of staggered micro-pin-fins. 2009 *Int. J. Heat Mass Transfer* **52**, 1853-1863.
[5] Wan W, Deng D, Huang Q, Zeng T, Huang Y. Experimental study and optimization of pin fin shapes in flow boiling of micro pin fin heat sinks. 2017 *Appl. Thermal Eng.* **114**, 436–449
[6] Lee YJ, Singh PK, Lee PS. Fluid flow and heat transfer investigations on enhanced microchannel heat sink using oblique fins with parametric study. 2015 *Int. J. Heat Mass Transfer* **81**, 325–336
[7] Kandlikar SG, Review and Projections of Integrated Cooling Systems for Three-Dimensional Integrated Circuits. 2014 *ASME J. Electronic Packag.* **136**, 024001
[8] Jang D, Yook S, Lee K, Optimum design of a radial heat sink with a fin-height profile for high-power LED lighting applications. 2014 *Appl. Energy* **116**, 260–268
[9] Marques C, Kelly KW. Fabrication and Performance of a Pin Fin Micro Heat Exchanger. 2004 *ASME J. Heat Transfer* **126**, 434-444
[10] Kosar A, Peles Y. Thermal-Hydraulic Performance of MEMS-based Pin Fin Heat Sink. 2006 *ASME J. Heat Transfer* **128**, 121-131
[11] Siu-Ho A, Qu W, Pfefferkorn F. Experimental Study of Pressure Drop and Heat Transfer in a Single-Phase Micro-Pin-Fin Heat Sink. 2009 ASME J. Electronic Packag. **129,** 479 -487.
[12] Jeng T, Tzeng S.Pressure drop and heat transfer of square pin-fin arrays in in-line and staggered arrangements. 2007 *Int. J. Heat Mass Transfer* **50,** 2364–2375.
[13] Roth R, Lenk G, Cobry K, Woias P. Heat transfer in freestanding microchannels with in-line and staggered pin fin structures with clearance. 2013 *Int. J. Heat Mass Transfer* **67**, 1–15
[14] Rasouli E, Naderi C, Narayanan V. Pitch and aspect ratio effects on single-phase heat transfer through microscale pin fin heat sinks. 2018 *Int. J. Heat Mass Transfer* **118**, 416–428
[15] Deng D, Tang Y, Liang D, He H, Yang S. Flow boiling characteristics in porous heat sink with reentrant microchannels. 2014 *Int. J. Heat Mass Transfer* **70**, 463–477
[16] Taylor JR. An Introduction to Error Analysis, second ed., University Science Books, 1997.
[17] Shen S, Xu JL, Zhou JJ, Chen Y. Flow and heat transfer in microchannels with srough wall surface. 2006 *Energy Conver. Manage.* **47**, 1311–1325